231098

UCRL-JC-126961
PREPRINT

Modeling of Bubble Dynamics in Relation to Medical Applications

P. A. Amendt, M. Strauss, R. A. London,
M. E. Glinsky, D. J. Maitland, P. M. Celliers,
S. R. Visuri, D. S. Bailey, D. A. Young,
and D. Ho

This paper was prepared for submittal to
SPIE Photonics West '97 Symposium
San Jose, California
February 8-14, 1997

March 12, 1997

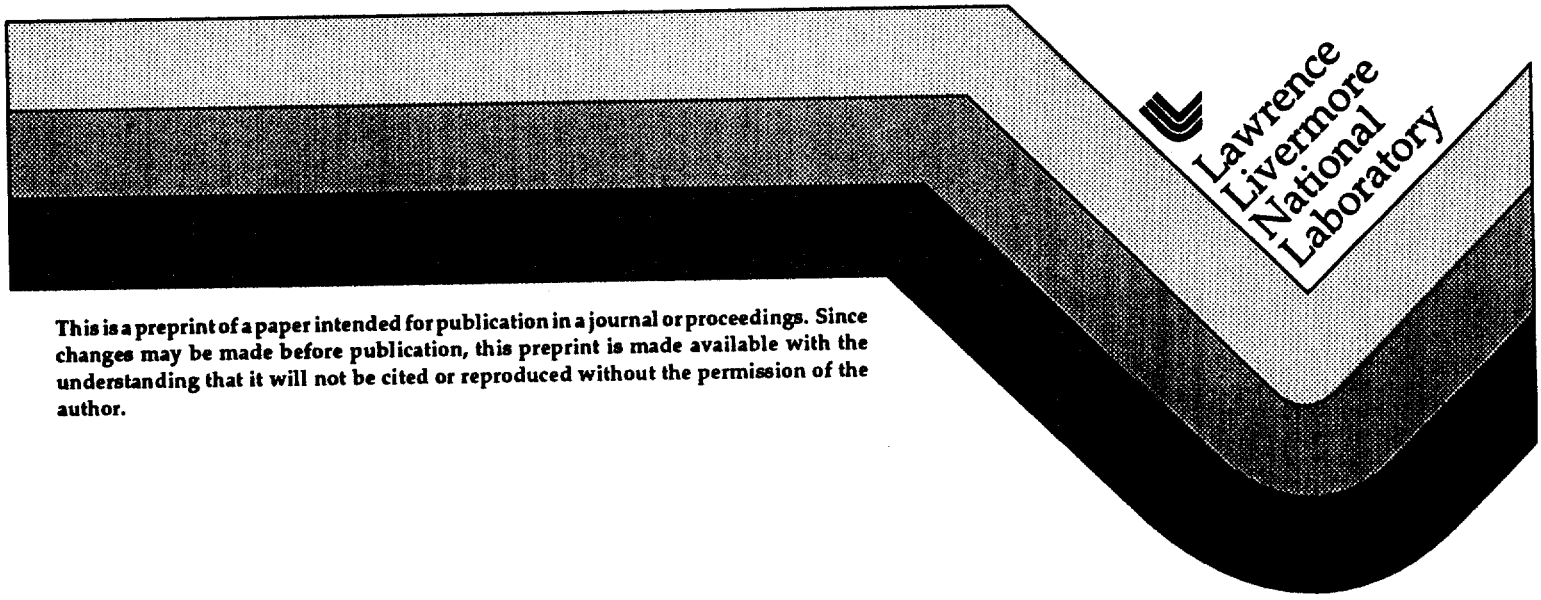

Modeling of bubble dynamics in relation to medical applications

P.A. Amendt, M. Strauss*, R.A. London, M.E. Glinsky, D.J. Maitland, P.M. Celliers, S.R. Visuri, D.S. Bailey, D.A. Young, and D. Ho

Lawrence Livermore National Laboratory, University of California, Livermore, CA 94550

**University of California at Davis and Nuclear Research Center, Bar Sheva, Israel*

Abstract

In various pulsed-laser medical applications, strong stress transients can be generated in advance of vapor bubble formation. To better understand the evolution of stress transients and subsequent formation of vapor bubbles, two-dimensional simulations are presented in channel or cylindrical geometry with the LATIS (LAser TISsue) computer code. Differences with one-dimensional modelling are explored, and simulated experimental conditions for vapor bubble generation are presented and compared with data.

I. Introduction

In many areas of pulsed-laser surgery, strong acoustic waves or shocks are initially generated which are followed by the formation of cavitation and vapor bubbles.[1] For example, laser-assisted coronary angioplasty is typically accompanied by the formation of vapor bubbles due to selective absorption of laser light by arterial thrombi.[2,3] In the vascular system, use of laser-generated bubbles is being considered as a possible means of disrupting an occlusion.[4] In the fields of opthalmology and dermatology, absorption of short-pulse laser light by melanin structures can produce damaging vapor bubbles.[5,6] For intraocular surgery, photodisruption of tissue is often accompanied by bubble generation which must be kept safely away from the retina and corneal endothelium.[7]

In medical applications the range of bubble formation occurs over a wide range of parameters. For example, the spatial dimensions of the irradiated tissue can range from 1 μm to 1 mm. Pulse lengths between 1 ps and 1 ms are available, and laser energies may range between 50 μJ and 100 mJ. The main theoretical tool available to researchers are Rayleigh-type models of bubble behavior which describe the evolution of the bubble radius $R(t)$ versus time t.[8] These Rayleigh-type models include the Rayleigh-Plesset equation, Gilmore equation, the Herring-Trilling equation, and the Kirkwood-Bethe equation.[8-11] All of these models implicity assume an initial low-density gaseous state which, however, is not the case during initial bubble expansion and latetime bubble collapse. At these instances, the density of the interior of

the bubble approaches that of a liquid, thereby invalidating a key assumption of Rayleigh-type modeling. During these brief stages of high bubble density when acoustic emission occurs, the energetics of vapor bubble evolution can be significantly impacted.

Recently, one-dimensional (1-d) hydrodynamic simulations have begun to be used for a more sophisticated treatment of bubble evolution, including the emission of acoustic radiation.[11-13] These studies have attempted to model the generation of vapor bubbles in experiments where the short-pulse laser energy is delivered via an optical fiber immersed in liquid.[14] Two key parameters in characterizing the bubble evolution are peak bubble size and time of peak expansion. Although the shape of the vapor bubble at maximum expansion is nearly round, the bubble evolution begins quite asymmetrically, due to the presence of the fiber behind the growing bubble. Comparing the simulated 1-d bubble growth with experiment is problematic because of the intrinsic, non-spherical geometry of the growing bubble. In this case, a two-dimensional (2-d) simulation is preferred in order to capture the strong deviations from spherical symmetry, particularly at early time.

The majority of experiments exploring vapor bubble evolution near a laser-irradiating fiber tip are conducted so that physical boundaries are well removed from the fiber tip.[14] In this way, the evolution of the vapor bubble is unaffected by reflecting shocks or acoustic waves for the duration of at least several cycles of bubble expansion and collapse. However, the evolution of vapor bubbles in a channel-like geometry such as an artery or large vessel can be susceptible to important 2-d effects which may appreciably affect bubble evolution. Use of a 2-d simulation code, such as LATIS[15], to investigate channel effects can be an important tool for understanding bubble dynamics in a realistic geometry.

In these Proceedings we review the status of 1-d modelling of bubble experiments for an effectively unbounded geometry. After comparing with experiment and noting some discrepancies, we turn our attention toward 2-d simulations. We find that the inclusion of non-radial flows in a 2-d calculation helps to reduce bubble expansion and to effect better agreement with the experiment. Finally, we discuss some preliminary work on simulating 2-d bubble evolution in a channel or vessel-like geometry.

2. One-dimensional modelling

A useful procedure for understanding observed vapor bubble behavior and deriving bubble scaling laws is through the use of 1-d hydrodynamic simulations.[12,13] The experiment that we concentrate on modelling consists of a 100 μm radius fiber optic tip immersed in an aqueous dye solution [See figure (1)]. The delivered half-micron wavelength energy is 0.317 mJ in 5 ns

with an exponential absorption profile $\exp[-\mu_a z]$ in the z-direction, or along the symmetry axis of the fiber. The absorption length μ_a^{-1} is 7 μm and the absorption profile is uniform in radius up to 100 μm. Beyond the radius of the fiber tip, the laser energy deposition is approximated by a Gaussian profile: $\exp[-\mu_r^2(r\text{-}100\mu m)^2]$, where μ_r is about 10 microns.

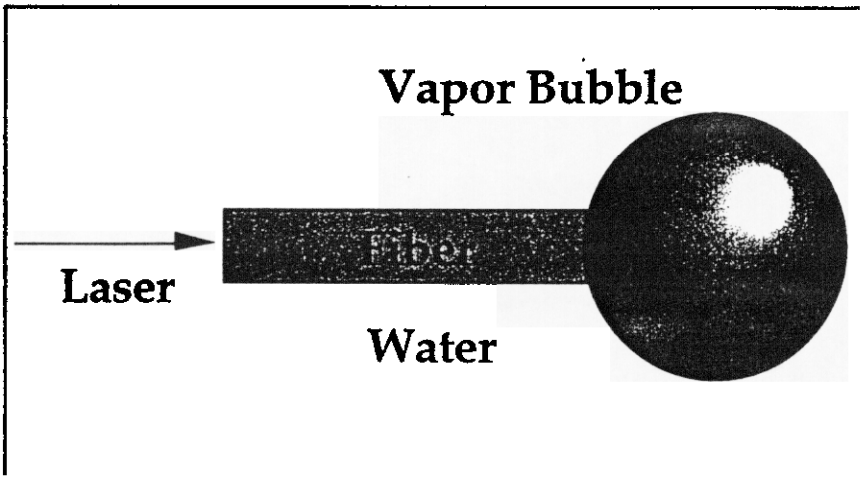

Fig. 1: Schematic of laser-generated vapor bubble experiment.

We use LATIS in 1-d geometry to model the average bubble growth versus time for these experimental conditions. The laser energy deposition is modeled by an effective energy source in the simulations which is constant in time during the pulse. The (spherical) absorption energy density profile $\xi(r)$ is chosen as

$$\xi(r) = \frac{E_0 \mu_a}{4\pi r^2} e^{-\mu_a (r - r_0)} , \qquad (1)$$

where E_0 is the total energy deposited and r_0 is the inner spherical radius of energy deposition. We choose r_0 so that the fiber tip surface area πr_f^2 matches the spherical surface area $4\pi r_0^2$. Thus, we deposit the energy in a spherical volume of inner radius 50 microns according to equation (1) in order to match both the surface area and heated volume of the (cylindrical) fiber tip.

Figure (2) shows a comparison of the experimental vapor bubble radius versus time with 1-d simulation results. One-dimensional simulations, in the manner described above, reproduce the qualitative bubble behavior and are very useful in large parameter studies and the development of scaling laws.[12,13] However, a significant quantitative discrepancy is evident between the 1-d modelling and data. A possible source of this difference may be related to the transition from a cylindrically symmetric energy deposition at early

time to nearly spherically symmetric bubble expansion at late time. Large transverse or nonradial flows can be initiated which represent an expenditure of energy that would otherwise go into bubble expansion. To understand the magnitude of nonradial effects, 2-d simulations must be undertaken.

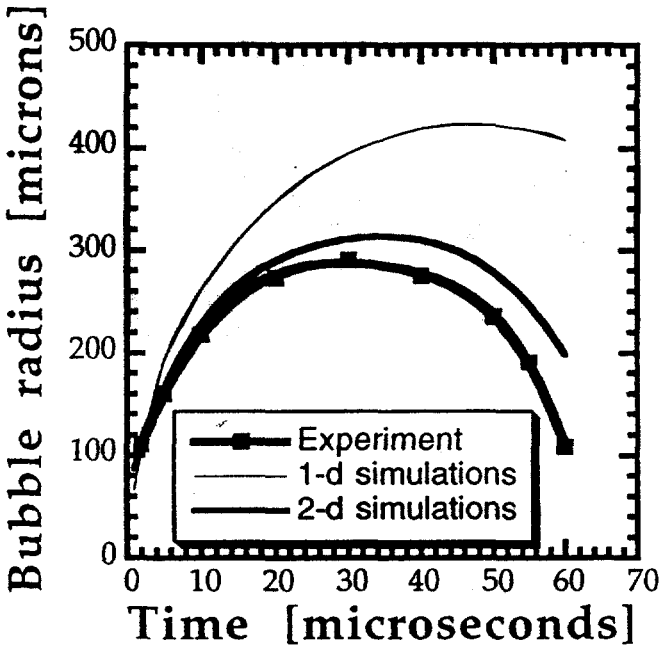

Fig. 2: Experimental and simulated bubble radii vs time. Energy is 0.317 mJ, absorption length is 7 μm, pulse length is 5 ns, and fiber radius is 100 μm.

3. Two-dimensional modelling

Consideration of 2-d modeling adds a significant degree of complexity compared with the 1-d simulations just discussed. While the choice of zonal mesh in 1-d calculations is straightforward, the two-dimensional case introduces a couple of choices. In particular, we must decide whether to use a Lagrangian scheme or an Eulerian algorithm for advecting the fluid. In the first case, the zonal mesh moves with the fluid, while in the latter scheme the fluid moves through a fix mesh. In the Lagrangian scheme, the mesh of quadrilateral zones can become so highly distorted that the simulation is not reliable or may cease altogether. In this case, some zones develop topological properties which we label as "boomeranged" and "bowtied". Figure (3) shows an example of a quadrilateral zone which successively evolves from a boomeranged shape to a bowtied configuration. For boomeranged zones, an artificial or numerical pressure is locally activated in order to attempt reversal of the boomeranging and prevent bowtying. Bowtying is more serious

because zonal quantities become multi-valued and lead to unreliable hydrodynamics. To avoid excessive occurrences of these problems, zonal remapping or rezoning is often used. In particular, the current mesh is overlayed by a previously saved mesh and the physical quantities of interest, such as energy and mass, are remapped onto the recorded mesh.

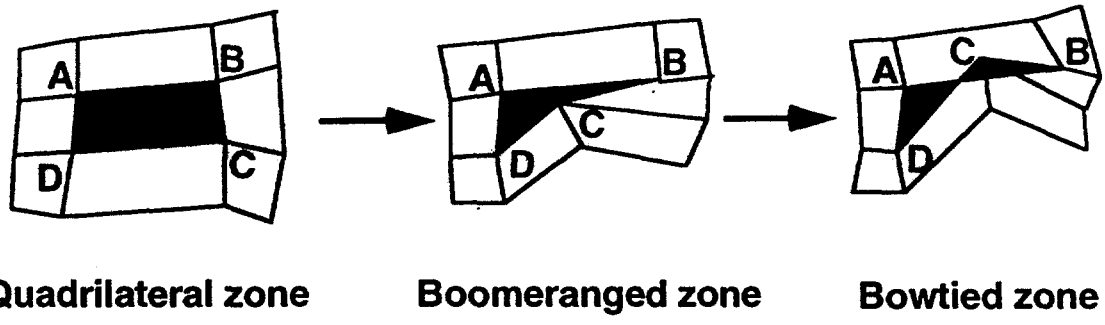

Fig. 3: Schematic evolution of a quadrilateral zone to a bowtied zone in a Lagrangian mesh. Points A, B, C, D represent vertices of shaded central zone.

We distinguish between two specific schemes for carrying out a 2-d simulation with LATIS. The first technique is termed "quasi-Lagrangian" and refers to allowing the mesh to evolve to a bowtied configuration before a remapping is required. In this scheme the mesh closely follows the fluid flow. The other technique is called "quasi-Eulerian" and refers to a remapping to a mesh which has been saved at an early time during the simulation. The main difference between the two schemes is that rezoning in the quasi-Lagrangian case involves a comparatively less drastic remapping of quantities when a remap is required. Consequently, the matching of mass between adjacent zones is better preserved in the quasi-Lagrangian mode. This feature is important for resolving the vapor-liquid interface which can separate regions of very disparate density. By contrast, the quasi-Eulerian approach tends to excessively smear the interface over time which may lead to unreliable hydrodynamics near the collapse phase of bubble evolution. However, a principal advantage of the quasi-Eulerian scheme is its relatively large hydrodynamic timestep per computational cycle and the resulting increase in speed.

For example, Figure (4) shows an example of a mesh for the two schemes at 5 μs. The small semicircle used at the corner of the fiber is for zoning purposes only and allows for more natural tracking of the bubble behind the fiber tip. In the quasi-Lagrangian case, the mesh is allowed to follow the fluid flow until a bowtie is encountered. Once a bowtied zone is detected, the simulation performs a remapping to a mesh which has been saved within the last microsecond. In this way, the mesh resolution is sufficiently fine near the vapor-liquid interface to well-resolve the bubble interface. Later in time, bowtying tends to occur within the vapor bubble region of the problem.

When this occurs, remapping is done in a manner which leaves the interface unperturbed and only the mesh within the bubble is manipulated to remove the bowtied zones. For the quasi-Eulerian case shown in Figure (4), more drastic remaps to an initial, nearly orthogonal mesh is performed. In this case, we also allow the simulation to continue until a zone bowties. The location of the bubble interface is evident from the perturbed mesh; however, the zonal resolution in this key region is clearly not as fine as in the quasi-Lagrangian case.

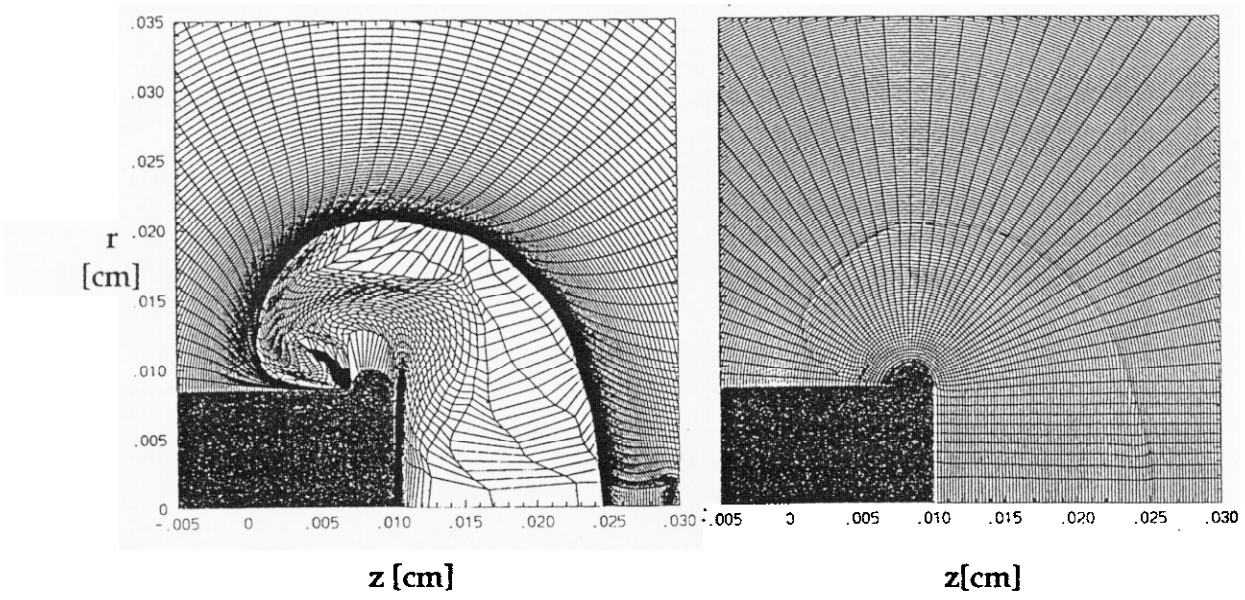

Fig. 4: Examples of zonal meshes at 5 μs for the (a) quasi-Lagrangian and (b) quasi-Eulerian schemes. Shown in the lower left-hand corner of each figure is the upper-half of the optical fiber with a maximum fiber radius of 100 μm.

In Figure (5) we show the fluid velocity field for the quasi-Lagrangian case at 1.4 μs. Note the presence of large velocities near and behind the corner of the fiber. Although a good deal of motion is evident in the vapor region of the bubble, the corresponding kinetic energy is not so large owing to the very low density of the vapor ($\approx 10^{-3}$ g/cm^3). What is noteworthy is the tendency of the zones just outside the bubble in the denser liquid region to move along the interface towards the back of the fiber. This non-radial component of motion is significant and represents a sink of energy which would otherwise go into radial bubble expansion. This feature represents an important difference between 1-d and 2-d simulation studies of vapor bubble evolution near a cylindrical fiber tip. In Figure (2) we show the average bubble radius obtained from the 2-d quasi-Lagrangian simulations alongside the data and 1-d simulations. A clear difference between the 1-d and 2-d simulations is evident, as well as the better agreement between experiment and the 2-d simulation results. Still, a discrepancy between the experimental maximum

bubble radius and the 2-d simulations remains. There are two possible sources for this remaining difference. First, we have not considered the presence of energy losses in the cladding surrounding the fiber which could reduce the amount of energy available for bubble expansion. Second, there is some evidence for photobleaching of the dye by the laser in the experiment. Rather than the 7 μm absorption length assumed in the simulations, a somewhat higher value may be realized. In support of this notion, recent interferometric measurements of density taken at early time in front of the fiber tip show a larger-than-expected absorption length.

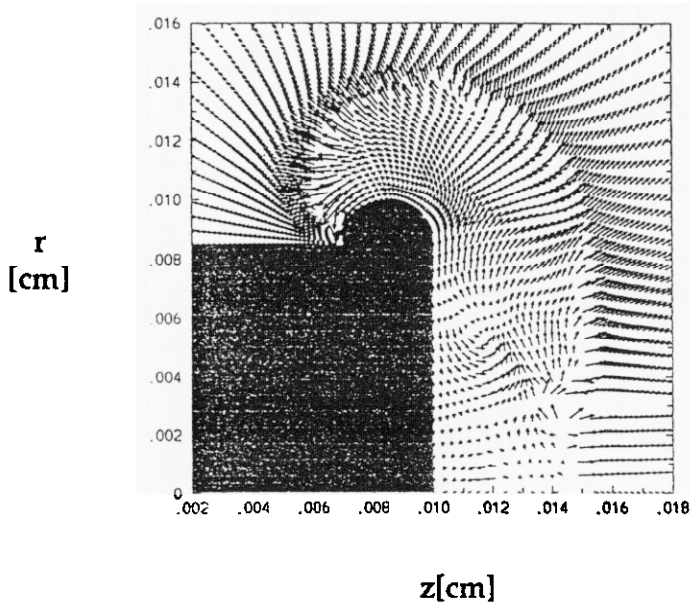

Fig. 5: The velocity field from the quasi-Lagrangian calculation at 1.4 μs. The largest velocity arrow corresponds to a speed of nearly 500 cm/s.

Finally, we consider bubble collapse and ask how well are we able to model this stage of late-time bubble evolution. In Figure (6) we show two shadowgrams of late time bubble evolution separated by 5 μs. Note the tendency of the bubble to pinch off in front of the fiber tip. This behavior may be related to an l=1 Rayleigh-Taylor instability seeded by the presence of the fiber,[16] where the integer l refers to the l-th Legendre mode in an expansion for the fluid variables. The l=1 mode corresponds to a left-right asymmetry in the bubble. The presence of the fiber naturally imposes such an asymmetry on the system. This l=1 symmetry breaking acts as a seed for hydrodynamic instability of the bubble during the deceleration phase of bubble collapse. The result is a characteristic "bubble" and "spike" form arising during the latter or nonlinear stages of Rayleigh-Taylor growth.[17] In figure (7) we show the simulated latetime images of the vapor bubble collapse stage obtained from a quasi-Lagrangian calculation. Qualitatively, a tendency of the collapsing bubble to pinch off as in the experiment is seen. The quasi-Lagrangian

calculation is used to track the latetime behavior in order to reduce the amount of Eulerian diffusion or smoothing characteristic of the quasi-Eulerian technique.

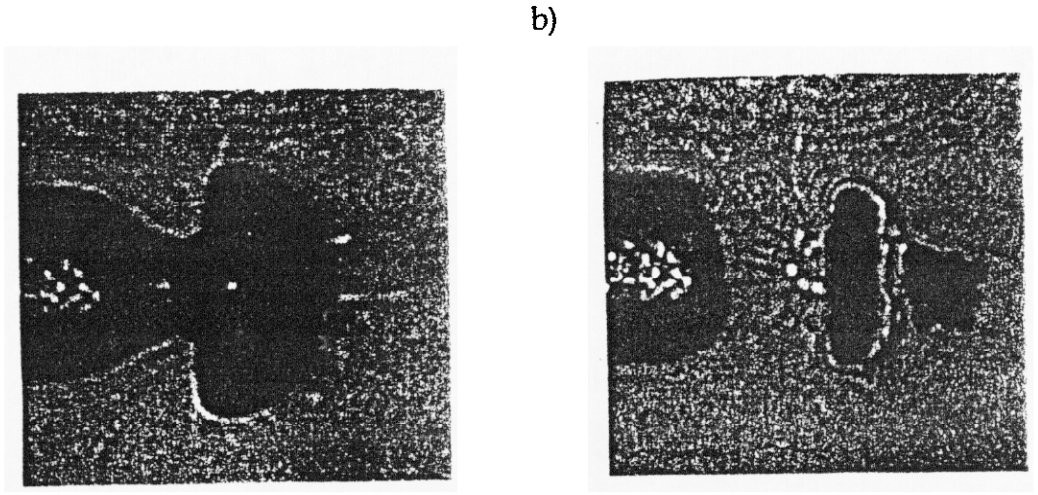

Fig. 6: Shown are two latetime experimental shadowgrams of the collapsing bubble. In (a), the time is 60 μs and in (b) 65 μs. The diameter of the fiber, including cladding, is 240 μm.

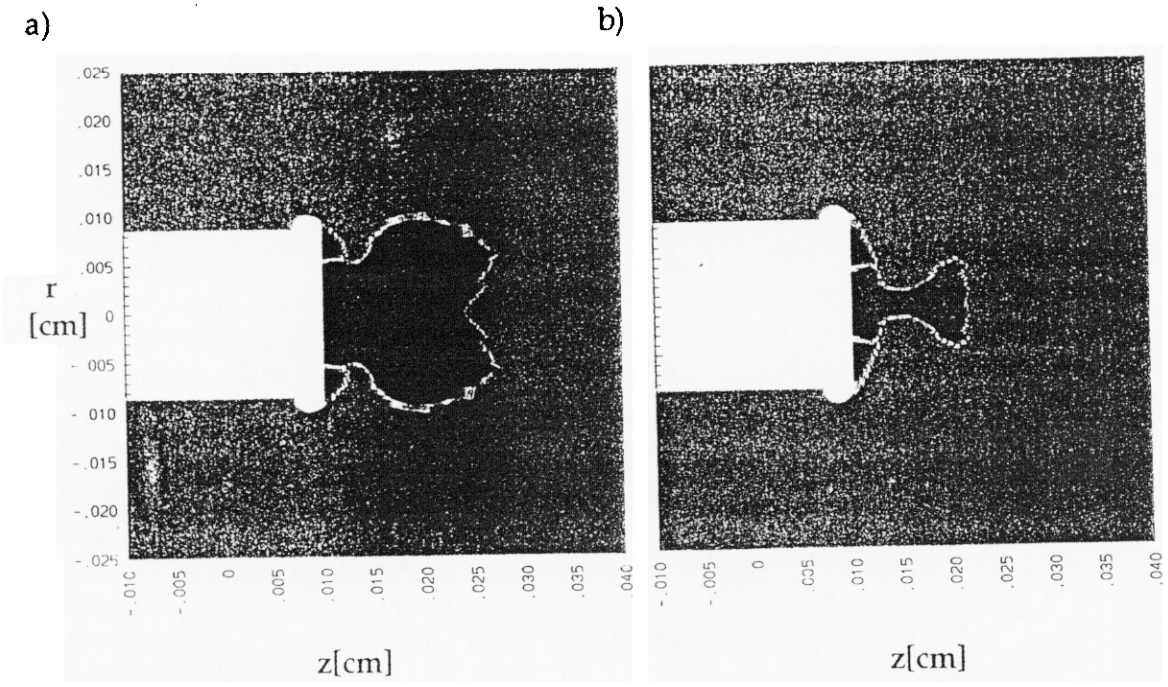

Fig. 7: Two latetime simulated bubble images at (a) 67 μs and (b) 68 μs. The fiber diameter is 200 μm.

4. Channel effects on vapor-bubble evolution

A more realistic study of 2-d bubble evolution must consider the effect of boundaries surrounding the laser-irradiated region. For example, the presence of vessel walls can have two consequences on vapor-bubble evolution. First, the acoustic impedance between blood and soft-tissue such as a vessel wall is not matched and may cause an acoustic wave to partially reflect back towards the fiber tip. The reflecting wave may be sufficiently strong near the axis of the vessel to disrupt the evolution of the vapor bubble. Second, a large vapor bubble may indeed approach the vessel boundary and undergo significant distortion as it continues to expand within the vessel.

We have begun to model the effect of channel boundaries on vapor bubble evolution. For the channel fluid we assume a two-phase equation-of-state (EOS) for water.[18] The vessel wall EOS is a scaled version of the water EOS, where the density is 20% higher but the sound speed is 10% lower compared to water. The acoustic impedance, or product of sound speed and density, is about 10% higher in the vessel material compared with the liquid. This level of impedance mismatch is intended to act as an upper bound compared with published values for a water-soft tissue interface.[19]

Shown in Figure (8) are the results of 2-d simulations with and without channel boundaries. For the former case, the boundary radius is 500 μm, and an ambient pressure of 10 atmospheres is used. Ongoing work shows that some of the effects of material strength can be crudely modeled by adopting a high ambient pressure in the failure-free calculations adopted here.[16] We consider only the case where the bubble dimension is a modest fraction of the channel radius in contrast to previous work.[3,20] For the example shown in Figure (8), the energy delivered in front of the fiber tip is 0.317 mJ as before [see Sections (2, 3)]. The influence of the partially reflecting acoustic wave from the vessel boundary on the evolving vapor bubble is seen to be weak in this case. A mild tendency for the confined bubble to grow more slowly is indicated, but the overall evolution appears to be little affected by the presence of a channel. Further calculations are in progress to assess the effect of a confining channel for a range of parameters, such as bubble energy and vessel radius.

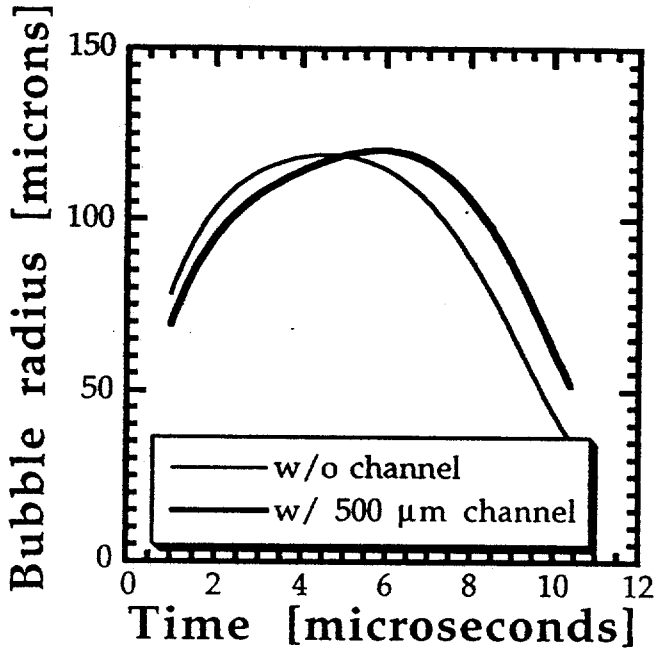

Fig. 8: Bubble radius vs time with channel (double solid line) and without channel (solid line). Radius of channel is 500 μm, fiber radius is 100 μm, ambient pressure is 10 atm, and energy delivered is 0.317 mJ over 5 ns.

5. Summary

We have begun modeling vapor bubble experiments with the LATIS simulation code. One-dimensional simulation studies predict significantly larger vapor bubbles and expansion times compared with experiment. Two-dimensional simulations show a significant amount of nonradial motion which is responsible for reduced bubble expansion. Thus, the 2-d simulations show much better agreement with data than the 1-d studies.

We are currently exploring various numerical algorithms to better track the vapor-liquid interface during the collapse phase. Qualitatively, we are able to reproduce some features observed in the experiment. Further development of our vapor bubble interface tracking will enable more reliable comparison with experiment during the collapse stage. Recent ArF laser and electric-discharge-induced vapor bubble generation experiments suggest the presence of forward-jetting immediately following collapse of the bubble.[21,22] Such hydrodynamic phenomena can have important ramifications for various laser-assisted vascular therapies.

Simulated bubble behavior in realistic channel geometries is currently under study. We have begun investigations of the role of a vessel boundary in vapor bubble evolution. Although we have not found a strong effect to date, further work is needed to explore the relevant parameter space.

6. Acknowledgments

This work was performed under the auspices of the U.S. Department of Energy by the Lawrence Livermore National Laboratory under contract W-7405-ENG-48. One of the authors (MEG) gratefully acknowledges the support of a U.S. Department of Energy Distinguished Postdoctoral Fellowship.

7. References

[1] T.G. van Leeuwen, E.D. Jansen, M. Motamedi, C. Borst and A.J. Welch, in *Optical-thermal response of laser irradiated tissue* (Edited by A.J. Welch and M.J.C. Van Gemert), p. 709. Plenum Press, New York, 1995.

[2] K. Gregory, in *Interventional Cardiology* (Edited by E.J. Topol), 2 892, W.B. Sanders Co., 1994.

[3] U. Sathyam, A. Shearin, and Scott Prahl, "Visualization of microsecond laser albation of procine clot and gelatin under a clear liquid", *Lasers in Surgery VI*, G.S. Abela and K.W. Gregory, Editors, Proc. SPIE **2671**, 28-35 (1996).

[4] U. Sathyam, A. Shearin, E. Chasteney, and Scott Prahl, "Threshold and ablation efficiency studies of microsecond ablation of gelatin underwater", *Lasers in Surgery and Medicine* **19**, 397-406 (1996).

[5] C.P. Lin and M.W. Kelly, in *Laser-Tissue Interaction VI* (Edited by S.L. Jacques), **2391**, 294 (1995).

[6] S.L. Jacques, R.D. Glickman, and J.G. Schwartz, in *Laser-Tissue Interaction VI*, (Edited by S.L. Jacques), **2391**, 468 (1996); S.L. Jacques, A.A. Oraevsky, R. Thompson, B.S. Gerstman, in *Laser-Tissue Interaction V* (Edited by S.L. Jacques), **2134A**, 54 (1994).

[7] A. Vogel and U. Parlitz, J. Acoust. Soc. Am. **100**, 148 (1996).

[8] L. Rayleigh, Philos. Mag. 34, 94 (1917).

[9] B.P. Barber and S.J. Putterman, Phys. Rev. Lett. 69, 3839 (1992).

[10] R.T. Knapp, J.W. Daily, and F.G. Hammitt, *Cavitation* (McGraw Hill, New York), p. 94 (1966).

[11] E.J. Chapyak and R.P. Godwin, in *Lasers in Surgery VI,*, G.S. Abela and K.W. Gregory, Editors, Proc. SPIE **2671**, 84 (1996).

[12] M. Strauss, P. Amendt, R.A. London, D.J. Maitland, M.E. Glinsky, P. Celliers, D.S. Bailey, D.A. Young, and S.L. Jacques, "Computational modeling of laser thrombolysis for stroke treatment", in *Lasers in Surgery VI,*, G.S. Abela and K.W. Gregory, Editors, Proc. SPIE **2671**, 11-21 (1996).

[13] M.E. Glinsky, P. Amendt, D.S. Bailey, R.A. London, and M. Strauss, "Rayleigh-type model of bubble evolution with material strength", in *Laser-Tissue Interaction VIII*, S.L. Jacques, Editor, Proc. SPIE **2975**, these Proceedings, (1997).

[14] P. Celliers, L.B. Da Silva, N.J. Heredia, B.M. Mammini, R.A. London, and M. Strauss, "Dynamics of laser-induced transients produced by nanosecond duration pulses", in *Lasers in Surgery VI*, G.S. Abela and K.W. Gregory, Editors, Proc. SPIE **2671**, 22 (1996).

[15] R.A. London, M.E. Glinsky, G.B. Zimmerman, D.S. Bailey, D.C. Eder, and S.L. Jacques, submitted to J. Appl. Optics: Optical Technology & Biomedical Optics (Feb., 1997).

[16] M.E. Glinsky, P.A. Amendt, D.S. Bailey, and R.A. London, "Rayleigh-type model of bubble evolution with material strength compared to detailed dynamic simulations", in*Laser Tissue-Interaction VIII*, S.L. Jacques, Editor, Proc. SPIE **2975**, these Proceedings (1997).

[17] J. Hecht, D. Ofer, U. Alon, D. Shvarts, S.A. Orszag, and R.L. McCrory, *Laser and Particle Beams* **13** (3), 423 (1995).

[18] L. Haar, J.S. Gallagher and G.S. Kell, *NBS/NRC Steam Tables*, McGraw-Hill, 1984.

[19] P.L. Carson, "Diagnostic ultrasound--physical principles and equipment", in *CRC Handbook of Medical Physics*, R.B. Waggener, J.G. Kereiakes, and R.J. Shalek, Editors, pp. 81-121. CRC Press, Inc., Boca Raton, Florida (1977); S.L. Jacques, A.A. Oraevsky, R. Thompson, and B.S. Gerstman, "A working theory and experiments on photomechanical disruption of melanosomes to explain the threshold for minimal visible retinal lesions for sub-ns laser pulses", in *Laser-Tissue Interaction V*, S.L. Jacques, Editor, Proc. SPIE **2134A**, 54-65 (1994).

[20] U. Sathyam, A. Shearin, and Scott Prahl, "Effects of spotsize, pulse energy and repetition rate on microsecond ablation of gelatin underwater", in *Laser-*

tissue Interaction VI, S.L. Jacques, Editor, Proc. SPIE **2391**, 336-344 (1995); U. Sathyam, A. Shearin, and Scott Prahl, "Investigations of basic ablation phenomena during laser thrombolysis", in *Lasers in Surgery VII*, K.W. Gregory, Editor, Proc. SPIE **2970**, in press (1997).

[21] I. Turovets, D. Palanker, Yu. Kokotov, I. Hemo and A. Lewis, "*Dynamics of cavitation bubble induced by 193 nm ArF excimer laser in concentrated sodium chloride solutions*", J. Appl. Phys. **79** (5), 1 (1996).

[22] D. Palanker, I. Turovets, and A. Lewis, "Electric discharge-induced cavitation: a competing approach to pulsed lasers for performing microsurgery in liquid media", in *Laser Tissue-Interaction VIII*, S.L. Jacques, Editor, Proc. SPIE **2975**, these Proceedings (1997).

Technical Information Department • **Lawrence Livermore National Laboratory**
University of California • Livermore, California 94551